ResearchGate

See discussions, stats, and author profiles for this publication at: https://www.researchgate.net/publication/279175915

Solvent Dependent Excited State Behaviors of Luminescent Gold(I)−Silver(I) Cluster with Hypercoordinated Carbon

ARTICLE *in* THE JOURNAL OF PHYSICAL CHEMISTRY C · JUNE 2015

Impact Factor: 4.77 · DOI: 10.1021/acs.jpcc.5b03985

READS

34

5 AUTHORS, INCLUDING:

Meng Zhou

Carnegie Mellon University

14 PUBLICATIONS **96** CITATIONS

SEE PROFILE

Qianjin Guo

Chinese Academy of Sciences

37 PUBLICATIONS **230** CITATIONS

SEE PROFILE

Available from: Meng Zhou

Retrieved on: 24 January 2016

THE JOURNAL OF PHYSICAL CHEMISTRY C

Article

pubs.acs.org/JPCC

Solvent Dependent Excited State Behaviors of Luminescent Gold(I)−Silver(I) Cluster with Hypercoordinated Carbon

Meng Zhou,[†] Zhen Lei,[‡] Qianjin Guo,[†] Quan-Ming Wang,*[,‡] and Andong Xia*[,†]

[†]Beijing National Laboratory for Molecular Sciences (BNLMS), Key Laboratory of Photochemistry, Institute of Chemistry, Chinese Academy of Sciences, Beijing 100190, People's Republic of China

[‡]State Key Laboratory of Physical Chemistry of Solid Surfaces, Department of Chemistry, College of Chemistry and Chemical Engineering, Xiamen University, Xiamen, Fujian 361005, People's Republic of China

Supporting Information

ABSTRACT: Polynuclear Au(I) complexes continues to attract considerable attention because of their bright emissions in the visible wavelength, which hold promise in applications in luminescence, fluorescence sensing, and bioimaging. Despite various spectroscopic investigations on their steady state properties, detailed understanding of the origin of their emissions and excited state relaxations is still lacking. Here, we report femtosecond time-resolved transient absorption experiments combined with quantum chemical calculations on a brightly emissive $[Au_6Ag_2(C)(dppy)_6](BF_4)_4$ cluster in different solvents. Global analysis on the transient absorption spectra based on a sequential model gives three spectral components: (1) excited state absorption (ESA) of $^1MLCT_{Au}$ state (τ = 1−3 ps); (2) ESA of $^3MLCT_{Au}$ state (τ = 11−40 ps), and (3) ESA of $^3MLCT_{Ag}$ state (long-lived). By variation of the solvent's polarity and hydrogen bonding ability, the relative population of the triplet MLCT states and the emission properties can be modulated. Especially in methanol, an additional site specific O−H···π bond is formed between methanol molecules and aromatic rings of ligands, which enhances the ultrafast nonradiative decay from the hydrogen bond stabilized $^3MLCT_{Au}$ state and reduces the population of the emissive $^3MLCT_{Ag}$ state. The results presented here about the excited state dynamics of luminescent gold(I)−silver(I) cluster allow a deeper insight into the origin of their emissions by monitoring the population of the emissive $^3MLCT_{Ag}$ state and dark $^3MLCT_{Au}$ state in different environments.

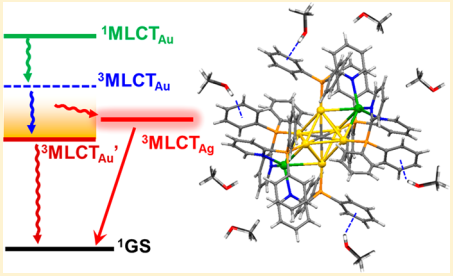

INTRODUCTION

Luminescent metal complexes are one of the most fascinating classes of complexes because of their possible applications in OLED display, fluorescence sensing, and biological labeling for imaging.[1−4] In particular, polynuclear Au(I) complexes have been widely investigated for their intense, long-lived emissions in the visible wavelength.[5−11] Au(I) has a closed-shell d^{10} electronic distribution and tends to aggregate through aurophilic interactions;[12,13] thus, organic ligands are generally used to form Au(I) complexes. Unlike those monolayer protected Au clusters with core and motif structure,[14−16] these complexes have the same number of metal atoms as ligands (homoleptic), with no core gold atoms.[17] The luminescence of Au(I) complexes originates from metal centered (MC), ligand-to-metal charge transfer (LMCT), metal to ligand charge transfer (MLCT), intraligand (IL), with aggregation through aurophilic interactions.[18−20] By introduction of appropriate coordinating ligands and bonding metal atoms such as Ag and Pt, the charge transfer dynamics as well as photophysical and spectroscopic properties of Au(I) complexes can easily be tuned. As efficient charge separation is a prerequisite for effective applications in photoexcitation energy and photocatalysis, a significant understanding of the origin of the emissions and excited state charge transfer dynamics on Au(I) complexes is indispensable for both fundamental research and their potential applications.

Metal-to-ligand charge transfer (MLCT) in the excited state of transition metal complexes has received considerable interest.[21−24] For Au(I) complexes coordinated with electron withdrawing ligands such as phosphines,[20,25] the steady state absorption exhibits MLCT bands that are sensitive to surrounding environments. As gold exhibits the strongest spin−orbital coupling, the excited state populations of Au(I) complexes will experience fast intersystem crossing into the low-lying triple state (about 1 ps). On the other hand, once the solute is excited, the surrounding solvent molecules will rearrange around the excited complexes according to the charge redistribution that accompanies photoexcitation and thus influences the reactivity of dissolved substrates.[26−30] As the time of solvent response is consistent with the intersystem crossing in gold(I) complexes (<1 ps),[23] the solvation dynamics may couple or otherwise influence the excited state dynamics of Au(I) complexes.[21,22] The photophysics of Au(I) complexes has been well investigated through steady state absorption and emission spectroscopy, whereas a fundamental understanding

Received: April 27, 2015
Revised: June 8, 2015

© XXXX American Chemical Society

DOI: 10.1021/acs.jpcc.5b03985
J. Phys. Chem. C XXXX, XXX, XXX−XXX

Scheme 1. Crystal Structure of $[Au_6Ag_2(C)(dppy)_6]^{4+}$ (A) and Simplified Optimized Structure of Ground State $[Au_6Ag_2(C)(PH_2py)_6]^{4+}$ (B)[a]

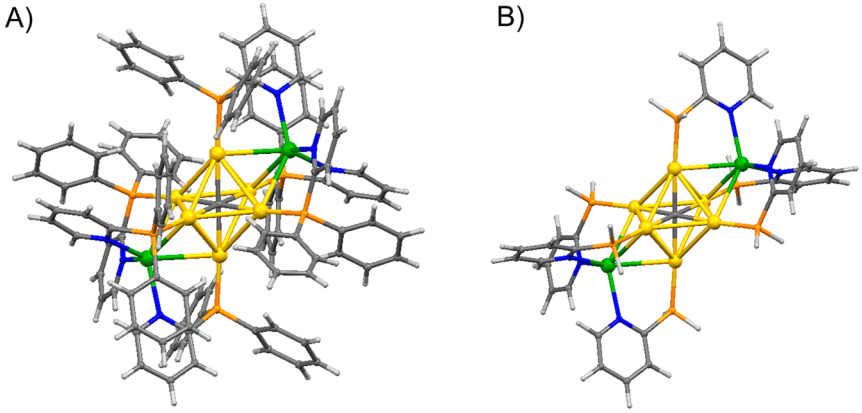

[a]Au atoms are colored yellow, Ag atoms green, N atoms blue, C atoms gray, P atoms orange, H atoms light gray.

of ultrafast solvent dependent excited state dynamics and relaxation mechanisms of Au(I) complexes is far from complete.

Here, to unravel and understand the real excited state dynamics of Au(I) complexes, we have investigated the excited state dynamics of a highly luminescent cluster $[Au_6Ag_2(C)(dppy)_6](BF_4)_4$ (**I**)[31] (Scheme 1) in three different solvents using femtosecond transient absorption spectroscopy combined with quantum chemical calculations. The carbon hypercoordinated cluster **I** contains an octahedral Au_6 core with two Ag atoms capping the two opposite Au_3 triangles and six peripheral diphenylphoshpino-2-pyridine (dppy) ligands. **I** is highly luminescent both in the solid state and in solution, which has been used to visualize the nucleolus of living cells[32] and to construct metal−organic frameworks (MOFs).[10] By using solvents with different polarity and hydrogen bonding ability (CH_2Cl_2, CH_3CN, CH_3OH), we are able to monitor the excited state dynamics and the electronic structure of **I** as a function of solvent properties. The steady state absorption spectra in the visible range are shifted by varying the solvent systems, while the emission wavelength remains unchanged. The gold(I)−silver(I) cluster exhibits ultrafast intersystem crossing rate (1−3 ps) and solvent dependent energy transfer, which gives rise to their different luminescent behaviors. Furthermore, the results suggest that the population of different states as well as the phosphorescence behaviors of gold(I)−silver(I) complexes can be modified in different solvents.

MATERIALS AND METHODS

Materials. The synthesis methods of $[Au_6Ag_2(C)(dppy)_6](BF_4)_4$ by Wang and co-workers were reported elsewhere.[31] Purified (kept in dark and low temperature) sample was dissolved in proper solvents (i.e., dichloromethane, acetonitrile, methanol) for spectroscopic measurements. All solvents were AR-grade.

Absorption and Emission Measurements. The steady state ultraviolet−visible (UV−vis) absorption was measured on a U3010 (Hitachi) spectrometer. The steady state emission and excitation spectra were measured using F4600 (Hitachi) fluorescence spectrometer. The lifetime of the emission is measured using a nanosecond flash photolysis setup in fluorescence mode (Edinburgh LP920, Edinburgh Instruments Ltd.), combined with a Nd:YAG laser (Surelite II, Continuum Inc.) at 355 nm as excitation wavelength.

Ultrafast Transient Absorption Spectra. The femtosecond transient absorption spectra were measured at ∼90 fs time resolution using a home-built femtosecond pump−probe setup, which has been described in detail elsewhere (see section S1 in Supporting Information).[33,34] Briefly, a 400 nm and 70 fs pulse generated by sum frequency generation was used as the pump beam, and a delayed white light continuum (WLC) generated from a 2-mm-thick water cell between 420 and 780 nm was used as the probe beam. A synchronized optical chopper was inserted into the pump beam path in order to record probe spectra that were classified as pumped and not-pumped spectra. Every spectrum was recorded 200 times, and the average spectrum was used in further data processing. About 90 nJ/pulse at 400 nm used for pumping was focused into the sample with a 110 μm spot. The polarizations of pump and probe beams were set to 54.7° for isotropy measurements.

Data Processing. Spectral chirp in the transient absorption spectra was corrected for group velocity dispersion of the probe beam before global fitting. The differential absorbance $\Delta A(t,\lambda)$ was analyzed using the population dynamics modeling graphical interface program Glotaran and TIMP.[35] $\Delta A(t,\lambda)$ is a superposition of different spectral components $\varepsilon_i(\lambda)$, weighted by their concentrations, $c_i(t)$:[36]

$$\Delta A(t,\lambda) = \sum_{i=1}^{n} c_i(t)\,\varepsilon_i(\lambda)$$

In the sequential model, the associated spectra are called evolution associated difference spectra (EADSs). In the target model, the associated spectra are termed species associated difference spectra (SADS) (see section S1 in Supporting Information).[35,36]

Quantum Chemical Calculation. Density function theory (DFT) was used to study the molecular orbitals and absorption spectra of the Au(I)−Ag(I) complexes. The quantum calculation of **I** was based on the structure reported by Wang et al.[31] For computing efficiency, the phenyl group in the dppy was replaced by H to form $[Au_6Ag_2(C)(PH_2py)_6]^{4+}$ (**II**). The stable ground state geometry of **II** was optimized using the PBE function with the LANL2DZ basis set for Au, Ag and the 6-31G(d,p) basis set for other atoms.[37,38] All the calculations were conducted by the method implemented in the Gaussian 03 program package.[39]

DOI: 10.1021/acs.jpcc.5b03985
J. Phys. Chem. C XXXX, XXX, XXX−XXX

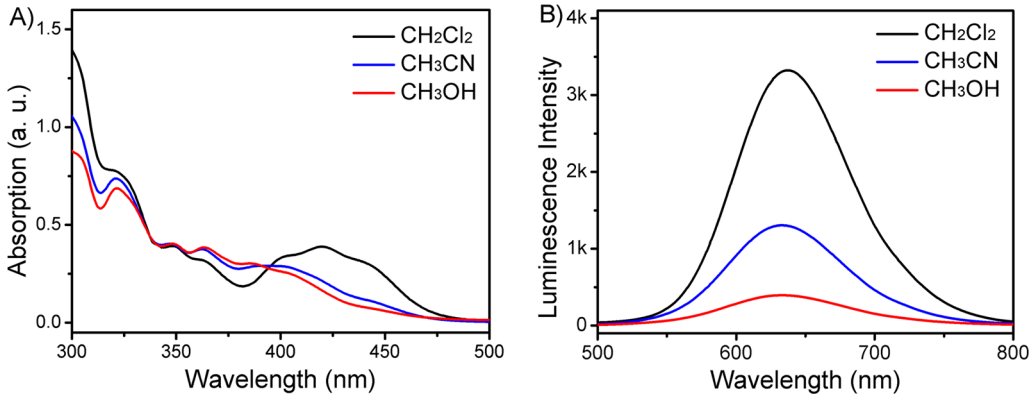

Figure 1. (A) Normalized steady state absorption spectra of **I** dissolved in three solvents, where the concentrations were adjusted to be the same (~8 × 10^{-5} mol/L) for all measurements. (B) Luminescence spectra of **I** with excitation of 350 nm in three solvents.

RESULTS AND DISCUSSIONS

Steady State Measurements. The steady state absorption spectra of **I** dissolved in CH_2Cl_2, CH_3CN, and CH_3OH are shown in Figure 1 A. To ensure the same concentration in three solvents, the sample was first dissolved in CH_2Cl_2 (~8 × 10^{-5} mol/L) and divided into three equal portions, which were then volatilized and dissolved in proper solvents of equal volume. In three solutions, similar absorption spectra were seen in the ultraviolet region while absorption of **I** in the visible region is relatively stronger in CH_2Cl_2 than that in CH_3CN and CH_3OH. The solvatochromic shift suggests that the visible absorption has charge transfer (CT) character,[40] while further assignment of the transitions requires quantum chemical calculations.

Luminescence of **I** was measured in three solutions with the same absorbance (~0.1 OD) at same excitation wavelength (350 nm). The emission spectra excited at 350 nm in all three solvents exhibit a monopeak around 640 nm with the intensity decreasing prominently from CH_2Cl_2 to CH_3CN and to CH_3OH (Figure 1B). Unlike the steady state absorption spectra, the steady state fluorescence excitation spectra monitoring the emission at 640 nm have almost the same spectral shape in three solvents after normalization (Figure S1). The emission spectra of **I** is less dependent on solvent than absorption spectra, which is a typical characteristic of MLCT transition.[40] The lifetime of the emission is much shorter in CH_3OH (1.6 μs) and CH_3CN (2.3 μs) than in CH_2Cl_2 (4.7 μs) (Figure S2). Besides, the luminescence quantum yield was measured to be about ~0.015, ~0.05, ~0.29 in CH_3OH, CH_3CN, CH_2Cl_2, respectively, with fluorescein in 0.1 mol/L NaOH aqueous solution as the standard (0.95).[41] The solvent dependent luminescence lifetimes and quantum yields suggest that radiationless transitions are stronger in the polar solvents because of the solvation effect. As the emission peaks of **I** have no shifts in different solvents, it is suggested that solvation has been completed before reaching the last emissive state. To get a deeper understanding of the electronic structure on **I**, quantum chemical calculation based on TDDFT was performed.

Quantum Chemical Calculations. Assignment of absorption band has been accomplished by TDDFT calculations as follows. The simulated linear absorption spectrum of **II** in CH_2Cl_2 was calculated using PCBM solvent model and an overall agreement besides a little blue shift is found compared with experiment (Figure 2A). Table 1 listed selected transition energies, oscillator strength, and the dominant orbital

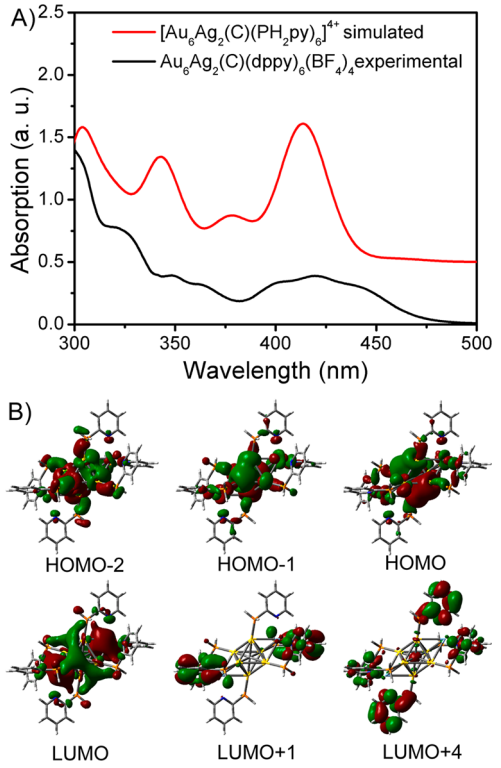

Figure 2. (A) Experimental and simulated linear absorptions of **I** in CH_2Cl_2. (B) Molecular orbitals associated with the ^{1}MLCT transitions based on TDDFT calculations.

Table 1. TDDFT Calculated Electronic Excitation Energies of $[Au_6Ag_2(C)(PH_2py)_6]^{4+}$

electronic transition	transition energy, eV (nm)	oscillator strengh	main orbital contribution
$S_0 \rightarrow S_1$	2.701 (459)	0.0035	HOMO → LUMO
$S_0 \rightarrow S_2$	2.702 (458)	0.0037	HOMO − 1 → LUMO
$S_0 \rightarrow S_3$	2.995 (413)	0.2924	HOMO − 2 → LUMO
$S_0 \rightarrow S_{14}$	3.283 (378)	0.0351	HOMO − 1 → LUMO + 1
$S_0 \rightarrow S_{15}$	3.288 (377)	0.0418	HOMO − 1 → LUMO + 4

contributions, while Figure 2B shows molecular orbitals involved in these transitions. Three occupied orbitals (HOMO, HOMO − 1, HOMO − 2) mainly consist of Au core orbitals, while the lowest and higher unoccupied orbitals

DOI: 10.1021/acs.jpcc.5b03985
J. Phys. Chem. C XXXX, XXX, XXX−XXX

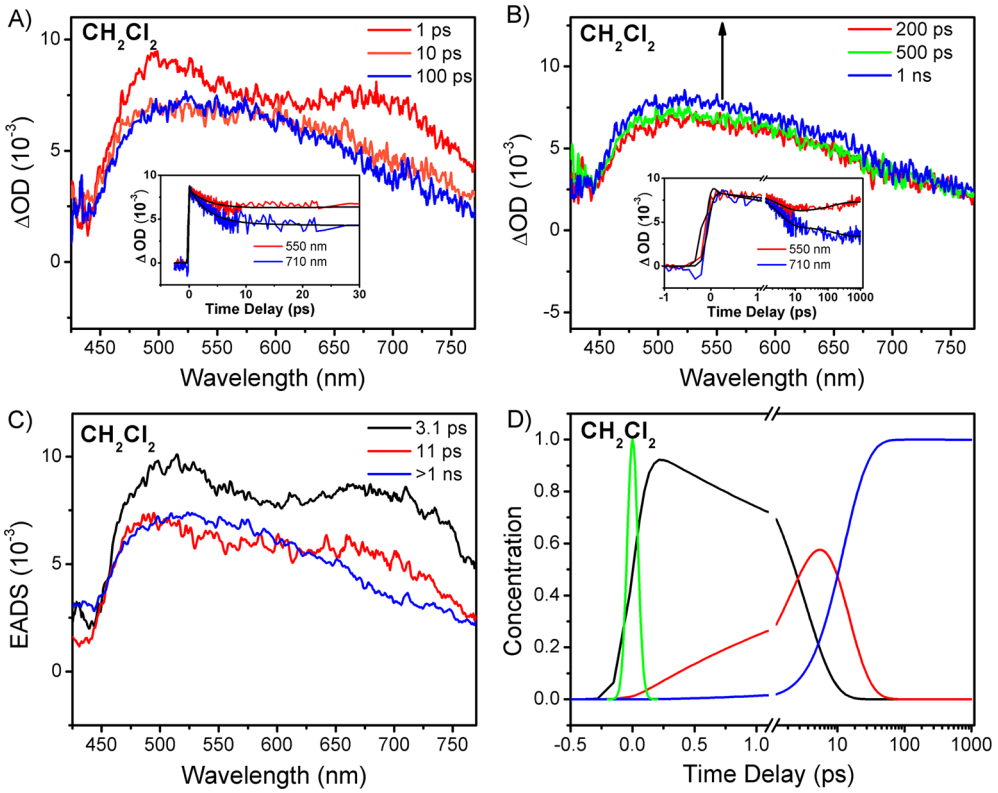

Figure 3. Femtosecond transient absorption spectra of **I** in CH_2Cl_2 (A) 0.2−2 ps and (B) 100 ps to 1 ns after excitation at 400 nm. (C, D) EADSs and concentrations of these components, where the green line stands for the instrument response. Insets of parts A and B represent the kinetics at selected wavelengths for showing the quality of global fitting.

Scheme 2. Relaxation Pathways of I in CH_2Cl_2 (A), CH_3CN (B), CH_3OH (C) after Excitation at 400 nm[a]

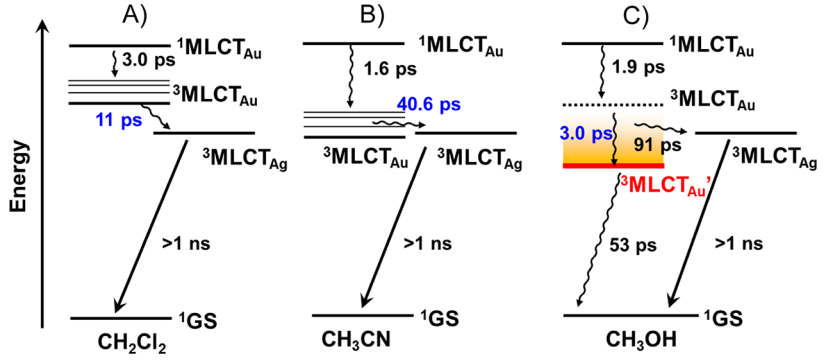

[a] $^3MLCT_{Au}'$ state represents a solvation and π−hydrogen bond stabilized MLCT state.

are localized on Ag atoms and the surface ligands, respectively. Therefore, the visible and ultraviolet absorptions of **I** can be ascribed to metal to ligand charge transfer (^{1}MLCT) band on Ag and Au atoms, respectively. Thus, 400 nm excitation selectively (though not solely) populates the $^1MLCT_{Au}$ state. To elucidate the origin of the luminescence and solvent dependent excited state manifold of **I**, ultrafast transient absorption spectroscopy of **I** was further carried out.

Ultrafast Transient Absorption Measurement. Parts A and B of Figure 3 show the femtosecond transient absorption spectra of **I** in CH_2Cl_2 at different time delays. Following excitation at 400 nm, ground state bleaching (GSB) at 425 nm $\leq \lambda_{probe} \leq$ 500 nm overlapping with broad excited state absorption (ESA) over the whole spectral region was observed. During the first few picoseconds, the ESA band around 700 nm decays rapidly to give rise to the ESA band around 500 nm (see Figure 3A and inset), suggesting the formation of a new intermediate state. After a 100 ps decay, the ESA around 500 nm begins to grow slowly during the rest of the measurement (>1 ns), which represents another very long-lived state (Figure 3B and inset). To figure out the relaxation mechanism, we analyzed the time-resolved absorption data using a sequential model with increasing lifetimes (1 → 2 → 3 → 4 ...) as shown in Scheme 2A. Figure 3C shows the evolution associated decay spectra (EADSs), and three lifetimes are required for an adequate fit of the data. Three time constants of 3.1 ps, 11 ps, and >1 ns were obtained from the global fitting. According to the calculation results described above, the first EADS is attributed to the ^{1}MLCT state on Au. It experiences intersystem crossing (3.1 ps) to the next EADS which

DOI: 10.1021/acs.jpcc.5b03985
J. Phys. Chem. C XXXX, XXX, XXX−XXX

Table 2. Emission Lifetimes and Global Fitting Parameters of EADS Obtained from fs-TA Spectra for I in Three Solvents after 400 nm Excitation in Various Solvents

solvent	ε [a]	α [b]	FL lifetime[c] (μs)	quantum yield	τ_1 (ps)	τ_2 (ps)	τ_3
CH_2Cl_2	8	0.22	4.7 ± 0.04	0.29 ± 0.01	3.1 ± 0.04	11 ± 0.1	>1 ns
MeCN	36.5	0.15	2.3 ± 0.02	0.05 ± 0.01	1.6 ± 0.03	40.6 ± 0.6	>1 ns
MeOH	35	0.98	1.6 ± 0.01	0.015 ± 0.01	1.9 ± 0.04	3 ± 0.06	53 ± 1 ps

[a]ε is the dielectric constant of the solvent from ref 26. [b]α characterizes the hydrogen bonding ability of the solvent, from ref 42. [c]The fluorescence (FL) lifetimes are obtained from the flash photolysis.

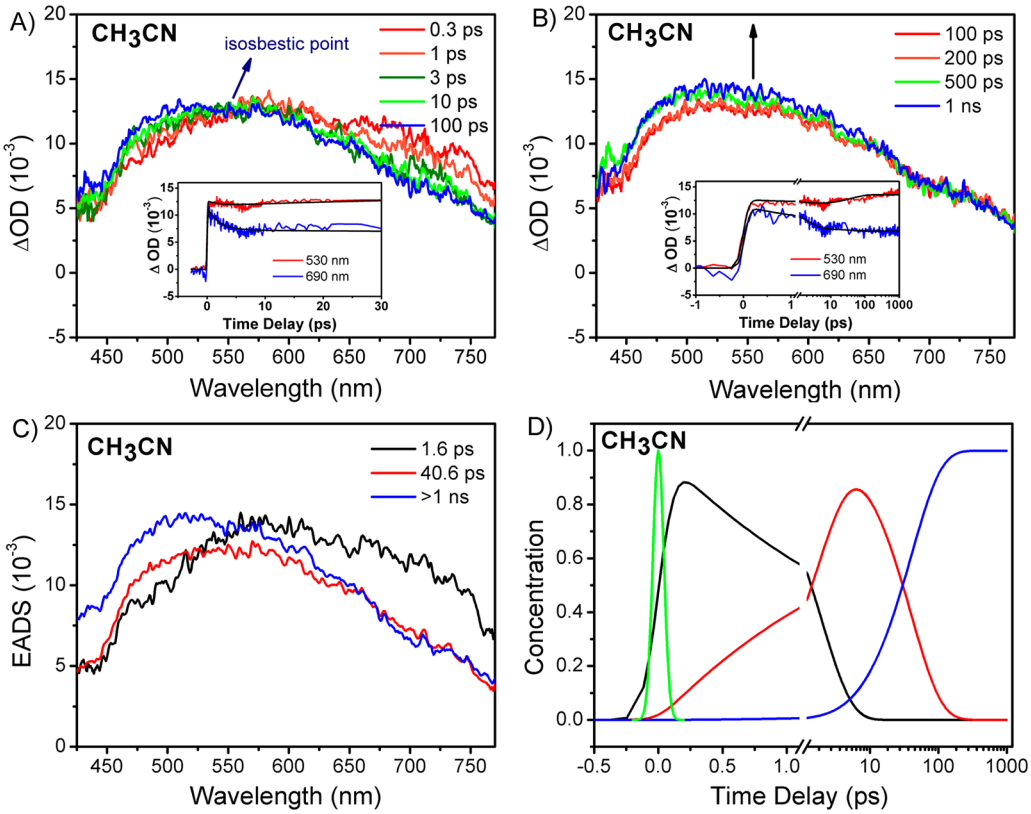

Figure 4. Femtosecond transient absorption spectra of **I** in CH_3CN (A) 0.3−100 ps and (B) 100 ps to 1 ns after excitation at 400 nm. (C, D) EADSs and concentrations of these components, where the green line stands for the instrument response. Insets of parts A and B represent the kinetics at selected wavelengths for showing the quality of global fitting.

represents the ^{3}MLCT state on Au. Regarding the solvent response time of CH_2Cl_2 (<1 ps),[26] the solvation process may couple to the intersystem crossing so that the resulting coupled solvation and intersystem crossing dynamics is 3.1 ps. The second EADS then evolves in 11 ps to the third EADS which represents the formation of the emissive triplet $^3MLCT_{Ag}$ state; i.e., the spectral evolution corresponds to the energy transfer process between $^3MLCT_{Au}$ and $^3MLCT_{Ag}$ triplet states. The relaxation model with corresponding time constants of **I** in CH_2Cl_2 is summarized in Scheme 2 A and in Table 2.

As changes in the nature of the solvent may have strong effect on the excited state processes of metal clusters,[33] we have investigated the excited state relaxation of **I** in more polar CH_3CN. As seen in Figure 4A, with increasing time delays, the ESA at 550 nm $\leq \lambda_{probe} \leq$ 750 nm decays to populate a new transient around 500 nm with an isosbestic point at 550 nm. The decay of the ESA at 680 nm correlates with the increase of the ESA at 500 nm (Figure 3A inset), suggesting the ultrafast transition of the excited state (^{1}MLCT on Au) to the intermediate state (^{3}MLCT on Au). At longer time delays, the evolution of ESA spectra of **I** in CH_3CN is similar to those measured in CH_2Cl_2 (Figure 4B), suggesting that energy level of the long-lived state is almost unaffected by changing the solvent polarity. The global fitting procedure gives three components with lifetimes of 1.6 ps, 40.6 ps, and >1 ns (Figure 4C,D), which represent the states of $^1MLCT_{Au}$, $^3MLCT_{Au}$, and $^3MLCT_{Ag}$, respectively. The relaxation model of **I** in CH_3CN is summarized in Scheme 2B, and the fitted parameters are listed in Table 2. Although the time of intersystem crossing from $^1MLCT_{Au}$ to $^3MLCT_{Au}$ remains almost unchanged, the energy transfer between $^3MLCT_{Au}$ and $^3MLCT_{Ag}$ states is much slower in CH_3CN (ε = 36.5) because of the stronger and faster solvation compared to that in less polar CH_2Cl_2 (ε = 8). It is clear that increasing the solvent polarity effectively decreases the quantum yield of the $^3MLCT_{Ag}$ state because of the strong competition between the solvation of $^3MLCT_{Au}$ and triplet−triplet energy transfer from $^3MLCT_{Au}$ to $^3MLCT_{Ag}$ states, which agrees with our steady state emission measurements.

Besides solvent polarity, hydrogen bonding also has a strong effect on excited state charge transfer dynamics.[43,44] Here, we addressed the question if and how the hydrogen bonding alters the excited state properties of metal−ligand complexes. In the

DOI: 10.1021/acs.jpcc.5b03985
J. Phys. Chem. C XXXX, XXX, XXX−XXX

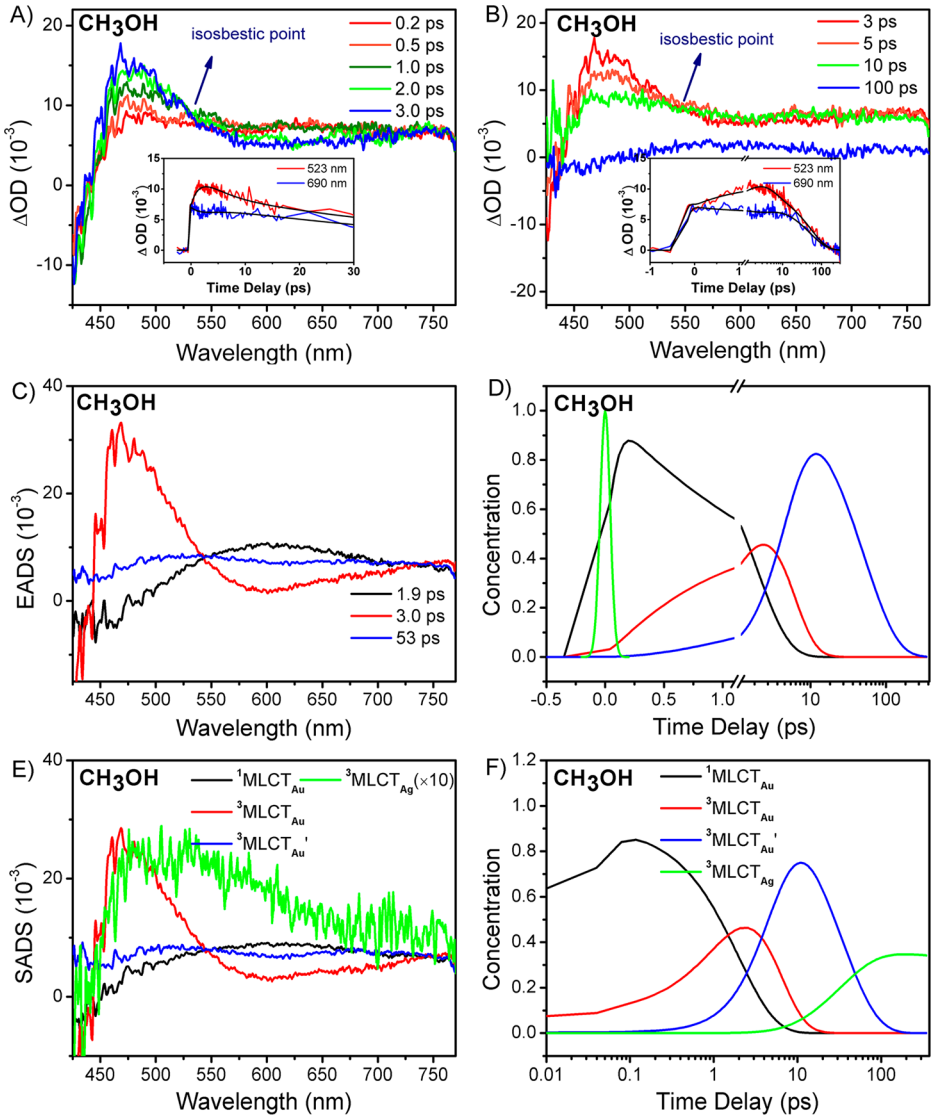

Figure 5. Femtosecond transient absorption spectra of **I** in in CH_3OH (A) 0.2−3 ps and (B) 3−100 ps after excitation at 400 nm. (C, D) EADSs and concentrations of these components, where the green line stands for the instrument response. (E, F) SADS and concentration of each species in the target model. Insets of parts A and B represent the kinetics at selected wavelengths for showing the quality of global fitting.

cluster **I**, there is no hydrogen acceptor, so it seems that no hydrogen bond can be formed in protic solvents. However, according to previous investigations, molecules with aromatic rings can form aromatic solute−(protic solvent)$_n$ clusters through π−hydrogen bond.[45,46] In this case, O−H···π H-bonds are formed as a result of the interaction between π electron density of the phenyl ring and the partially positively charged hydrogen of OH. Therefore, it is of great importance to investigate the effect of π−hydrogen bond on the excited state dynamics of **I** in protic solvent. Compared with MeCN (ε = 36.5), MeOH has similar polarity (ε = 35) but much stronger hydrogen bonding ability;[25] thus, we investigate the effect of hydrogen bonding by repeating the femtosecond transient absorption measurements of **I** in methanol.

In MeOH, entirely different excited state features were obtained. The ESA between 550 and 750 nm decays rapidly to form a stronger ESA around 470 nm in the first 3 ps (Figure 5A). The isosbestic point at 550 nm indicates the generation of a new transient, which, according to the analysis above, is ascribed to the ^{3}MLCT$_{Au}$ state. In the following 10 ps, there is an increase in the ESA at 600 nm and a significant decrease of the signal at 480 nm (Figure 5B), giving the same isosbestic point at 550 nm. Unlike those measured in CH_2Cl_2 and MeCN, the broad ESA then decays to zero in less than 100 ps. From the global fitting results as shown in Figure 5C and Figure 5D, it is found that the first EADS in MeOH is similar to that in MeCN while stronger ESA around 480 nm was observed in the second EADS in MeOH (Figure 5C). Similar to that in MeCN, the first two EADSs are ascribed to the ^{1}MLCT$_{Au}$ state and ^{3}MLCT$_{Au}$ state, respectively. Unlike those long-lived and nondecay EADSs in CH_2Cl_2 and MeCN, the third EADS component is formed rapidly and the fitting gives no long-lived component (see Figure 5D). As MeOH has strong hydrogen bonding ability, in addition to the normal solvation of free MeOH around excited state **I**, the last short-lived EADS (53 ps) could further be related to the hydrogen bonding, where the solvation from free MeOH together with the additional solvent effects of bound MeOH via π−hydrogen bonding leads to a remarkable decrease of potential surface of the finally relaxed ^{3}MLCT$_{Au}$ state.

DOI: 10.1021/acs.jpcc.5b03985
J. Phys. Chem. C XXXX, XXX, XXX−XXX

During the global analysis, EADS suggests that the population decays in a sequential pathway, which is used to determine the minimum number of exponentials needed to fit the data.[36] For **I** in methanol, the population decays in a nonsequential manner so that these EADSs are actually a combination of different excited states.[47] To further resolve the pure excited state species, we performed the target global analysis based on the model in Scheme 2C. Four species associated difference spectra (SADS) were then obtained (see Figure 5E,F). The spectral shapes of the first three SADS are similar to those of the EADSs in Figure 5C, while the last SADS has a spectral shape similar to that of the third EADS in CH_2Cl_2 and CH_3CN which represents the emissive $^3MLCT_{Ag}$. Therefore, these four SADSs represent $^1MLCT_{Au}$, $^3MLCT_{Au}$, solvation, and π−hydrogen bond stabilized $^3MLCT_{Au}$ (termed as $^3MLCT_{Au}{}'$ state) and $^3MLCT_{Ag}$ state, respectively. As $^3MLCT_{Au}$ state is further stabilized in CH_3OH, less than 30% of the excited state population is transferred to $^3MLCT_{Ag}$ state in 91 ps (see Figure 5F), which leads to the lowest emission quantum yield (0.015) in three solvents.

To confirm the presence of O−H···π bond in methanol, nuclear magnetic resonance (NMR) measurement was performed by adding methanol or methanol mixed with **I** complexes into CD_2Cl_2 (see Figure 6), respectively. The NMR

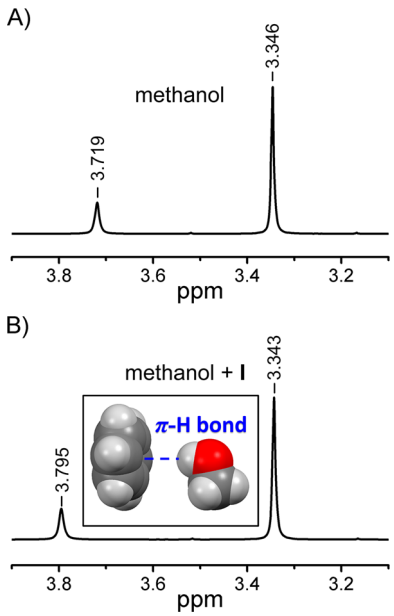

Figure 6. ^1H NMR spectra of (A) CH_3OH (16%) and (B) CH_3OH(16%) mixed with $[Au_6Ag_2(C)(dppy)_6](BF_4)_4$ (1 mg). All of the measurements were performed in CD_2Cl_2. Inset of part B shows the scheme of π−hydrogen bond between the aromatic rings of **I** and methanol molecules.

analysis was performed on a Bruker Avance 400 spectrometer operating at 400.1 MHz for ^1H. During the measurement, the NMR signal of hydrogen of −OH on methanol in CD_2Cl_2 was monitored as comparison. In Figure 6, the ^1H signal around 3.7−3.8 is assigned to the −OH group while the ^1H signal around 3.34 is from the $-CH_3$ group. After $[Au_6Ag_2(C)(dppy)_6](BF_4)_4$ (1 mg) was added to the methanol/CD_2Cl_2 mixture, the chemical shift of hydrogen on OH group was increased from 3.719 to 3.795. The chemical shift was increased by 0.08, which is due to the shielding effect of hydrogen bonding.[48] The result from NMR indicates the presence of intermolecular O−H···π bond between OH group on methanol and phenol rings on $[Au_6Ag_2(C)(dppy)_6](BF_4)_4$.

Furthermore, from Scheme 2 and Table 2, it is found that the intersystem crossing from $^1MLCT_{Au}$ state to $^3MLCT_{Au}$ occurs in a few picoseconds, almost unchanged in all three solutions. This is due to the similar response time of three solvents,[26] which strongly coupled to the intersystem crossing. Since triplet states have different dipole moments with singlet states, solvation will continuously proceed after the intersystem crossing. Thus, both singlet and triplet $MLCT_{Au}$ states will be stabilized by solute−solvent interactions. In CH_3CN, the clusters experience stronger solvent reaction and the $^3MLCT_{Au}$ state is further stabilized by solvent during solvation; thus, the energy level of the stabilized $^3MLCT_{Au}$ state will finally be equal or even lower than that of $^3MLCT_{Ag}$. Meanwhile, during solvation of $^3MLCT_{Au}$ state with the decreasing potential energy surface, the energy transfer from $^3MLCT_{Au}$ to $^3MLCT_{Ag}$ occurs simultaneously with less population of $^3MLCT_{Ag}$ since the solvation is very fast in polar solvents. As a result, the energy transfer from $^3MLCT_{Au}$ to $^3MLCT_{Ag}$ is significantly slower in CH_3CN (40.3 ps) than that in CH_2Cl_2 (11 ps). The energy difference between the $^3MLCT_{Au}$ and $^3MLCT_{Ag}$ may vary as a function of solvent polarity, thus altering the rate of the energy transfer between these two states (see Table 2 and Scheme 2). In methanol solution, besides the solvation from free methanol molecules around the cluster through dipole−dipole interaction, there is quite an amount of methanol molecules that already bind to the phenyl rings of **I** via π−hydrogen bond even at ground state (see inset of Figure 6B). Upon photoexcitation, not only free solvent dipoles but solvent dipole molecules bound through π−hydrogen bond will all rearrange themselves around the cluster surface so that solvation in methanol will be further enhanced, leading to even lower energy level of the stabilized $^3MLCT_{Au}$ state than that of $^3MLCT_{Ag}$. Solvation enhanced by the additional π−hydrogen bonding can further facilitate the nonradiation deactivation which competes significantly with energy transfer from $^3MLCT_{Au}$ state to $^3MLCT_{Ag}$ state, resulting in much slower $^3MLCT_{Au}$ state to $^3MLCT_{Ag}$ energy transfer and less population of $^3MLCT_{Ag}$ state. Meanwhile, as the $^3MLCT_{Au}$ state is further stabilized in acetonitrile and methanol, population of the emissive $^3MLCT_{Ag}$ state is remarkably quenched through competition between triplet state energy transfer and solvation, which leads to the decreasing emission quantum yield (see Table 2). On the basis of the results described above, it is suggested that the emission quantum yield of the gold(I)−silver(I) complexes significantly depends on the degree of solvation of both singlet and triplet of $MLCT_{Au}$ states. Moreover, it should be mentioned that, as shown in Figure 1B, the emission spectra of Au(I)−Ag(I) clusters in such three solvents remain the same except for changes of fluorescence quantum yields. Since the average solvent reorganization times of the three solvents used in our work are all very fast at less than 5 ps or even faster,[26] this may mainly result from the fast solvation only around $MLCT_{Au}$. According to the quantum chemical calculations, 400 nm excitation mainly populates the $^1MLCT_{Au}$ state and solvation after excitation has completed in several picoseconds before the excited state energy evolves to the $^3MLCT_{Ag}$ state from $^3MLCT_{Au}$, since the triplet−triplet energy transfer occurs in tens of picoseconds as determined in our work (see Scheme 2). On the other hand, the excited state solvation should strongly occur when the molecule was excited with large excess energy

DOI: 10.1021/acs.jpcc.5b03985
J. Phys. Chem. C XXXX, XXX, XXX−XXX

and large dipole moment change in excited state relative to that of its ground state. Therefore, as an acceptor of triplet−triplet energy transfer for $^3MLCT_{Ag}$ state from $^3MLCT_{Au}$, there is less solvation for $^3MLCT_{Ag}$ so that the energy level of $^3MLCT_{Ag}$ is almost unchanged, and emission maximum exhibits no shift in the three solvents.

To probe the impact of silver atom on the emission properties of gold(I) complexes, we have also investigated the ultrafast relaxation dynamics of $[Au_6(C)(dppy)_6](BF_4)_2$ for comparison. Details of the femtosecond transient absorption spectroscopy on the gold(I) complexes is shown in section S5 of Supporting Information. For gold(I) complexes without Ag atoms, the relaxation pathway is dominated by intersystem crossing from $^1MLCT_{Au}$ to $^3MLCT_{Au}$ which is short-lived and weakly luminescent in solution. On the basis of the results discussed here, introduction of silver atoms to the gold(I) complexes increases the luminescence quantum yield, where the emission occurs from the long-lived "bright" $^3MLCT_{Ag}$ state rather than the short-lived "dark" $^3MLCT_{Au}$ state.

CONCLUSION

In summary, the experimental and theoretical calculation results suggest that the luminescence of Au_6Ag_2 clusters originates from the low lying $^3MLCT_{Ag}$ state. By using ultrafast pump−probe spectroscopy combined with global analysis, we have drawn a significant picture of the excited state processes of **I** for intersystem crossing and energy transfer pathway as a cascade model: $^1MLCT_{Au} \rightarrow {}^3MLCT_{Au} \rightarrow {}^3MLCT_{Ag}$. The intersystem crossing process from $^1MLCT_{Au}$ to $^3MLCT_{Au}$ which occurred in a few picoseconds is coupled with solvation. Moreover, the energy transfer from $^3MLCT_{Au}$ to $^3MLCT_{Ag}$ and the luminescence quantum yield can be tuned by controlling the solvent polarity and hydrogen bonding ability. Especially in methanol, NMR results confirmed the existence of additional site specific O−H···π bond between methanol and phenyl rings on the ligands of **I**. As a result, the emission is largely quenched because of nonradiative deactivation from the additional π−hydrogen bond stabilized $^3MLCT_{Au}$ state ($^3MLCT_{Au}'$ state). The current work provides a deeper understanding of the solvent dependent emission properties and photophysics of gold(I) complexes through gold(I)−silver(I) interactions and the solvation of both singlet and triplet $^3MLCT_{Au}$ states. These results are helpful to the rational design of these homoleptic ligand protected gold(I) clusters with increasing applications in emitters, OLED display, and sensing.

ASSOCIATED CONTENT

Supporting Information

Details of transient absorption spectroscopy, data analysis, steady state excitation spectra, emission lifetimes, ^1H NMR of the gold complexes, and the transient absorption spectra and analysis of gold(I) complexes. The Supporting Information is available free of charge on the ACS Publications website at DOI: 10.1021/acs.jpcc.5b03985.

AUTHOR INFORMATION

Corresponding Authors

*Q.-M.W.: e-mail, qmwang@xmu.edu.cn.
*A.X.: e-mail, andong@iccas.ac.cn

Notes

The authors declare no competing financial interest.

ACKNOWLEDGMENTS

This work was supported by the 973 Program (Grant 2013CB834604), NSFC (Grants 21173235, 21125102, 21127003, 21333012, and 21373232), and the Strategic Priority Research Program of the Chinese Academy of Sciences (Grant XDB12020200).

REFERENCES

(1) Ma, Y.; Che, C.-M.; Chao, H.-Y.; Zhou, X.; Chan, W.-H.; Shen, J. High Luminescence Gold(I) and Copper(I) Complexes with a Triplet Excited State for Use in Light-Emitting Diodes. *Adv. Mater.* **1999**, *11*, 852−857.
(2) Baldo, M. A.; Thompson, M. E.; Forrest, S. R. Phosphorescent Materials for Application to Organic Light Emitting Devices. *Pure Appl. Chem.* **1999**, *71*, 2095−2106.
(3) Sánchez-Barragán, I.; Costa-Fernández, J. M.; Sanz-Medel, A.; Valledor, M.; Campo, J. C. Room-Temperature Phosphorescence (RTP) for Optical Sensing. *TrAC, Trends Anal. Chem.* **2006**, *25*, 958−967.
(4) Lo, K. K.-W.; Hui, W.-K.; Chung, C.-K.; Tsang, K. H.-K.; Ng, D. C.-M.; Zhu, N.; Cheung, K.-K. Biological Labelling Reagents and Probes Derived from Luminescent Transition Metal Polypyridine Complexes. *Coord. Chem. Rev.* **2005**, *249*, 1434−1450.
(5) Schmidbaur, H. Ludwig Mond Lecture. High-Carat Gold Compounds. *Chem. Soc. Rev.* **1995**, *24*, 391−400.
(6) Mansour, M. A.; Connick, W. B.; Lachicotte, R. J.; Gysling, H. J.; Eisenberg, R. Linear Chain Au(I) Dimer Compounds as Environmental Sensors: A Luminescent Switch for the Detection of Volatile Organic Compounds. *J. Am. Chem. Soc.* **1998**, *120*, 1329−1330.
(7) Wang, Q.-M.; Lee, Y.-A.; Crespo, O.; Deaton, J.; Tang, C.; Gysling, H. J.; Concepción Gimeno, M.; Larraz, C.; Villacampa, M. D.; Laguna, A.; Eisenberg, R. Intensely Luminescent Gold(I)−Silver(I) Cluster Complexes with Tunable Structural Features. *J. Am. Chem. Soc.* **2004**, *126*, 9488−9489.
(8) Yam, V. W.-W.; Cheng, E. C.-C. Highlights on the Recent Advances in Gold Chemistry—A Photophysical Perspective. *Chem. Soc. Rev.* **2008**, *37*, 1806−1813.
(9) Fernández, E. J.; López-de-Luzuriaga, J. M.; Monge, M.; Olmos, M. E.; Pérez, J.; Laguna, A.; Mohamed, A. A.; Fackler, J. P. $\{Tl[Au(C_6Cl_5)_2]\}_n$: A Vapochromic Complex. *J. Am. Chem. Soc.* **2003**, *125*, 2022−2023.
(10) Lei, Z.; Pei, X.-L.; Jiang, Z.-G.; Wang, Q.-M. Cluster Linker Approach: Preparation of a Luminescent Porous Framework with NbO Topology by Linking Silver Ions with Gold(I) Clusters. *Angew. Chem., Int. Ed.* **2014**, *53*, 12771−12775.
(11) Hau, F. K.-W.; Lee, T. K.-M.; Cheng, E. C.-C.; Au, V. K.-M.; Yam, V. W.-W. Luminescence Color Switching of Supramolecular Assemblies of Discrete Molecular Decanuclear Gold(I) Sulfido Complexes. *Proc. Natl. Acad. Sci. U.S.A.* **2014**, *111*, 15900−15905.
(12) Pyykkö, P. Strong Closed-Shell Interactions in Inorganic Chemistry. *Chem. Rev.* **1997**, *97*, 597−636.
(13) Che, C.-M.; Lai, S.-W. Luminescence and Photophysics of Gold Complexes. In *Gold Chemistry*; Mohr, F., Ed.; Wiley-VCH: Weinheim, Germany, 2009; pp 249−281.
(14) Qian, H.; Zhu, M.; Wu, Z.; Jin, R. Quantum Sized Gold Nanoclusters with Atomic Precision. *Acc. Chem. Res.* **2012**, *45*, 1470−1479.
(15) Jin, R. Quantum Sized, Thiolate-Protected Gold Nanoclusters. *Nanoscale* **2010**, *2*, 343−362.
(16) Templeton, A. C.; Wuelfing, W. P.; Murray, R. W. Monolayer-Protected Cluster Molecules. *Acc. Chem. Res.* **1999**, *33*, 27−36.
(17) Stamplecoskie, K. G.; Kamat, P. V. Size-Dependent Excited State Behavior of Glutathione-Capped Gold Clusters and Their Light-Harvesting Capacity. *J. Am. Chem. Soc.* **2014**, *136*, 11093−11099.
(18) Yam, V. W.-W.; Lo, K.K.-W. Luminescent Polynuclear d^{10} Metal Complexes. *Chem. Soc. Rev.* **1999**, *28*, 323−334.

DOI: 10.1021/acs.jpcc.5b03985
J. Phys. Chem. C XXXX, XXX, XXX−XXX

(19) Forward, J. M.; Bohmann, D.; Fackler, J. P.; Staples, R. J. Luminescence Studies of Gold(I) Thiolate Complexes. *Inorg. Chem.* **1995**, *34*, 6330−6336.
(20) Delfs, C. D.; Kitto, H. J.; Stranger, R.; Swiegers, G. F.; Wild, S. B.; Willis, A. C.; Wilson, G. J. Photoluminescence Properties of Four-Coordinate Gold(I)−Phosphine Complexes of the Types $[Au(diphos)_2]PF_6$ and $[Au_2(tetraphos)_2](PF_6)_2$. *Inorg. Chem.* **2003**, *42*, 4469−4478.
(21) Yeh, A. T.; Shank, C. V.; McCusker, J. K. Ultrafast Electron Localization Dynamics Following Photo-Induced Charge Transfer. *Science* **2000**, *289*, 935−938.
(22) McCusker, J. K. Femtosecond Absorption Spectroscopy of Transition Metal Charge-Transfer Complexes. *Acc. Chem. Res.* **2003**, *36*, 876−887.
(23) Vogt, R. A.; Gray, T. G.; Crespo-Hernández, C. E. Subpicosecond Intersystem Crossing in Mono- and Di(organophosphine)-gold(I) Naphthalene Derivatives in Solution. *J. Am. Chem. Soc.* **2012**, *134*, 14808−14817.
(24) Kuimova, M. K.; Alsindi, W. Z.; Blake, A. J.; Davies, E. S.; Lampus, D. J.; Matousek, P.; McMaster, J.; Parker, A. W.; Towrie, M.; Sun, X.-Z.; et al. Probing the Solvent Dependent Photophysics of fac-$[Re(CO)_3(dppz\text{-}X_2)Cl]$ (dppz-X_2 = 11,12-X_2-dipyrido[3,2-a:2′,3′-c]-phenazine); X = CH_3, H, F, Cl, CF_3). *Inorg. Chem.* **2008**, *47*, 9857−9869.
(25) Tlahuice-Flores, A.; Whetten, R. L.; Jose-Yacaman, M. Ligand Effects on the Structure and the Electronic Optical Properties of Anionic $Au_{25}(SR)_{18}$ Clusters. *J. Phys. Chem. C* **2013**, *117*, 20867−20875.
(26) Horng, M. L.; Gardecki, J. A.; Papazyan, A.; Maroncelli, M. Subpicosecond Measurements of Polar Solvation Dynamics Coumarin 153 Revisited. *J. Phys. Chem.* **1995**, *99*, 17311−17337.
(27) Fleming, G. R.; Cho, M. H. Chromophore-Solvent Dynamics. *Annu. Rev. Phys. Chem.* **1996**, *47*, 109−134.
(28) Zheng, J.; Kwak, K.; Asbury, J.; Chen, X.; Piletic, I. R.; Fayer, M. D. Ultrafast Dynamics of Solute-Solvent Complexation Observed at Thermal Equilibrium in Real Time. *Science* **2005**, *309*, 1338−1343.
(29) Gong, Y.; Guo, X.; Wang, S.; Su, H.; Xia, A.; He, Q.; Bai, F. Photophysical Properties of Photoactive Molecules with Conjugated Push−Pull Structures. *J. Phys. Chem. A* **2007**, *111*, 5806−5812.
(30) Jia, M.; Ma, X.; Yan, L.; Wang, H.; Guo, Q.; Wang, X.; Wang, Y.; Zhan, X.; Xia, A. Photophysical Properties of Intramolecular Charge Transfer in Two Newly Synthesized Tribranched Donor−π−Acceptor Chromophores. *J. Phys. Chem. A* **2010**, *114*, 7345−7352.
(31) Jia, J.-H.; Wang, Q.-M. Intensely Luminescent Gold(I)−Silver(I) Cluster with Hypercoordinated Carbon. *J. Am. Chem. Soc.* **2009**, *131*, 16634−16635.
(32) Chen, M.; Lei, Z.; Feng, W.; Li, C.; Wang, Q.-M.; Li, F. A Phosphorescent Silver(I)−Gold(I) Cluster Complex that Specifically Lights Up the Nucleolus of Living Cells with FLIM Imaging. *Biomaterials* **2013**, *34*, 4284−4295.
(33) Zhou, M.; Vdović, S.; Long, S. R.; Zhu, M. Z.; Yan, L. Y.; Wang, Y. Y.; Niu, Y. L.; Wang, X. F.; Guo, Q. J.; Jin, R. C.; et al. Intramolecular Charge Transfer and Solvation Dynamics of Thiolate-Protected $Au_{20}(SR)_{16}$ Clusters Studied by Ultrafast Measurement. *J. Phys. Chem. A* **2013**, *117*, 10294−10303.
(34) Zhou, M.; Long, S.; Wan, X.; Li, Y.; Niu, Y.; Guo, Q.; Wang, Q.-M.; Xia, A. Ultrafast Relaxation Dynamics of Phosphine-Protected, Rod-Shaped Au_{20} Clusters: Interplay between Solvation and Surface Trapping. *Phys. Chem. Chem. Phys.* **2014**, *16*, 18288−18293.
(35) Snellenburg, J. J.; Laptenok, S. P.; Seger, R.; Mullen, K. M.; van Stokkum, I. H. M. lotaran: A Java-Based Graphical User Interface for the R Package TIMP. *J. Stat. Software* **2012**, *49*, 1−22.
(36) van Stokkum, I. H. M.; Larsen, D. S.; van Grondelle, R. Global and Target Analysis of Time-Resolved Spectra. *Biochim. Biophys. Acta, Bioenerg.* **2004**, *1657*, 82−104.
(37) Perdew, J. P.; Burke, K.; Ernzerhof, M. Generalized Gradient Approximation Made Simple. *Phys. Rev. Lett.* **1996**, *77*, 3865−3868.
(38) Pei, Y.; Gao, Y.; Shao, N.; Zeng, X. C. Thiolate-Protected $Au_{20}(SR)_{16}$ Cluster: Prolate Au_8 Core with New $Au_3(SR)_4$ Staple Motif. *J. Am. Chem. Soc.* **2009**, *131*, 13619−13621.
(39) Frisch, M. J.; Trucks, G. W.; Schlegel, H. B.; Scuseria, G. E.; Robb, M. A.; Cheeseman, J. R.; Scalmani, G.; Barone, V.; Mennucci, B.; Petersson, G. A.; et al. *Gaussian 03*, revision E.01; Gaussian, Inc.: Wallingford, CT, 2004.
(40) Chen, P.; Meyer, T. J. Medium Effects on Charge Transfer in Metal Complexes. *Chem. Rev.* **1998**, *98*, 1439−1478.
(41) Lakowicz, J. R. *Principles of Fluorescence Spectroscopy*, 3rd ed.; Springer: New York, 2006.
(42) Airinei, A.; Homocianu, M.; Dorohoi, D. O. Changes Induced by Solvent Polarity in Electronic Absorption Spectra of Some Azo Disperse Dyes. *J. Mol. Liq.* **2010**, *157*, 13−17.
(43) Mohammed, O. F. Ultrafast Intramolecular Charge Transfer of Formyl Perylene Observed Using Femtosecond Transient Absorption Spectroscopy. *J. Phys. Chem. A* **2010**, *114*, 11576−11582.
(44) Zhao, G.-J.; Han, K.-L. Hydrogen Bonding in the Electronic Excited State. *Acc. Chem. Res.* **2011**, *45*, 404−413.
(45) Matisz, G.; Kelterer, A.-M.; Fabian, W. M. F.; Kunsági-Máté, S. Coordination of Methanol Clusters to Benzene: A Computational Study. *J. Phys. Chem. A* **2011**, *115*, 10556−10564.
(46) Zwier, T. S. The Spectroscopy of Aolvation in Hydrogen-Bonded Aromatic Clusters. *Annu. Rev. Phys. Chem.* **1996**, *47*, 205−241.
(47) Zhu, J.; Vreede, J.; Hospes, M.; Arents, J.; Kennis, J. T. M.; van Stokkum, I. H. M.; Hellingwerf, K. J.; Groot, M. L. Short Hydrogen Bonds and Negative Charge in Photoactive Yellow Protein Promote Fast Isomerization but Not High Quantum Yield. *J. Phys. Chem. B* **2015**, *119*, 2372−2383.
(48) Litwinienko, G.; Megiel, E.; Wojnicz, M. Hydrogen Bonding between Phenols and Fatty Acid Esters: ^1H NMR Study and ab Initio Calculations. *Org. Lett.* **2002**, *4*, 2425−2428.

DOI: 10.1021/acs.jpcc.5b03985
J. Phys. Chem. C XXXX, XXX, XXX−XXX